GEOPHYSICAL RESEARCH LETTERS, VOL. 26, NO. 11, PAGES 1609-1612, JUNE 1, 1999

How and why climate variability differs between the tropical Atlantic and Pacific

Shang-Ping Xie[1], Youichi Tanimoto[2], Hideyuki Noguchi[1], and Taroh Matsuno[2]

Abstract. The tropical Pacific and Atlantic Oceans share many common climatological features such as easterly trade winds, eastward shoaling thermocline, an eastern cold tongue and a northerly intertropical convergence zone (ITCZ). However, a comparison of climate variability between the two oceans reveals more differences than similarities. The Pacific is dominated by the equatorially symmetric El Nino/Southern Oscillation (ENSO) while the Atlantic ITCZ is controlled by changes in interhemispheric sea surface temperature (SST) gradient. To understand the causes of these differences in variability, a dynamic ocean-atmosphere coupling model is developed that includes both the Bjerknes and wind-evaporation-SST feedbacks. Equatorially symmetric and anti-symmetric modes emerge from the model, displaying distinct growth rate dependence on zonal wavenumber. Consistent with observations, an equatorially trapped ENSO mode dominates an ocean with a longitudinal size of the Pacific while in a smaller Atlantic-size one, a monopole mode with a broad meridional scale coexists with an equatorially anti-symmetric dipole mode.

1. Observational Background

The detection and understanding of physical modes of climate variability are important because they provide the much needed predictability. There seems a general consensus that more than one modes of SST variability exist in the tropical Atlantic. What these modes are is still under much debate. Some (Servain 1991; Nobre and Shukla 1996; Chang et al. 1997) argue that they consist of an equatorial-symmetric interannual monopole akin to the Pacific ENSO and an anti-symmetric decadal dipole, whereas some others (Houghton and Tourre 1992; Enfield and Mayer 1997; Mehta 1998), noting a lack of interhemispheric correlation in SST, suggest instead a combination of northern and southern tropical modes. Given the shortness of reliable data record and the nonlinearity of the system, an unambiguous empirical determination of tropical Atlantic modes does not seem to come by soon. Physical modeling is therefore necessary to corroborate empirical evidence. Here we take such a combined empirical-physical approach, whose results converge and favor a monopole-dipole decomposition of the Atlantic variability. Our modeling results further provide clues as to why the dipole mode is more visible in the Atlantic than in the Pacific.

We divide the Atlantic basin into two separate parts north and south of the equator, and compute empirical orthogonal functions (EOFs) of SST variability in each sub-basin separately. This eliminates the problem of artificial interhemispheric correlation that an EOF analysis over the whole Tropics may force (Houghton and Tourre 1992). Choosing 5°N—the latitude of the ITCZ—as the boundary for these subdomains does not change the results. SST anomalies are averaged for the boreal winter (November-April)—the time when SST variance is at the maximum—and filtered through an 8-16-year frequency band to extract decadal variability. The leading EOFs for the North and South Atlantic (NA & SA) both display meridionally stacked action centers of alternate polarities (Fig. 1), consistent with previous

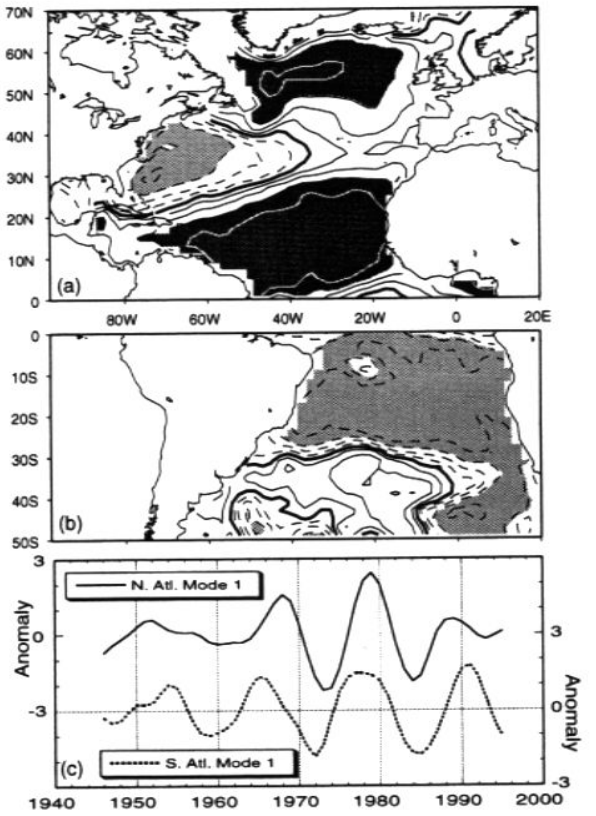

Figure 1 The first SST EOFs for **a**, the North and **b**, the South Atlantic, which explain 43.4% and 44.2% of band-passed variance in their respective sub-basins. **c**, Their time series, with which the correlation coefficient at each grid point is shown in **a** and **b** (contour interval: 0.2; zero contour thickened; >0.6 shaded). The GISST dataset is used, but the COADS gives similar results.

[1] Graduate School of Environmental Earth Science, Hokkaido University, Sapporo, Japan
[2] Frontier Research System for Global Change, Tokyo, Japan

Paper number 1999GL900308.
0094-8276/99/1999GL900308$05.00

analyses in these subdomains (Deser and Blackmon 1993; Kushnir 1994; Venegas et al. 1997).

Here the leading NA and SA EOFs are derived from independent samples so that there is no *a priori* reason for them to be correlated. Yet piecing Figs. 1a and 1b together reveals that they form a dipole in the Tropics with action centers of opposing polarities across the equator. Moreover their time series are correlated (Fig. 1c), with the correlation coefficient (0.64) exceeding the 95% significance level of a 8-freedom t-test. The strong time-space coherence across the equator indicates that the independently obtained NA and SA EOFs in fact represent a single Pan Atlantic Decadal Oscillation (PADO) mode, of which the tropical dipole is an integral part (Xie and Tanimoto 1998). Counter-intuitive but in support of the inter-hemispheric linkage, the variance associated with the SA dipole peaks in boreal winter when extratropical NA variability and atmospheric teleconnection are both strongest (not shown).

Paired with the dipole is a monopole mode that tends to vary on interannual time scales and displays the same polarity over the whole tropical Atlantic (Servain 1991). Both the monopole and dipole have strong bearings on rainfall variability over the surrounding continents. Particularly, northeast Brazil rainfall is correlated with interhemispheric SST gradient (Nobre and Shukla 1996), displaying a quasi-decadal regularity (Mehta 1998) suggestive of the working by a physical mode. Indeed, observed decadal oscillation in interhemispheric SST gradient can be simulated in a coupled model that includes the dipole physics and is forced by extratropical winds (Xie and Tanimoto 1998).

Unfiltered SST variability is known to be poorly correlated between the northern and southern tropical Atlantic (Fig. 2). While implying the existence of more than one modes in the Atlantic, the decorrelation of unfiltered SST variability between the tropical NA and SA does not necessarily mean their physical independence. The monopole-dipole pair, with comparable amplitudes but distinct time scales (Servain 1991; Houghton and Tourre 1992; Tanimoto and Xie 1999), can also lead to an apparent interhemispheric decorrelation.

Let us consider the time evolution of a positive SST anomaly localized within the northern Tropics as in Fig. 2. The atmosphere responds by generating significant southerly wind anomalies across the equator (thick curve), which can further induce anomalous zonal winds in the SA and initiate interhemispheric interactions. How such a hemispherically confined SST anomaly evolves with time requires an understanding of coupled ocean-atmosphere dynamics, on which we focus in the rest of the paper.

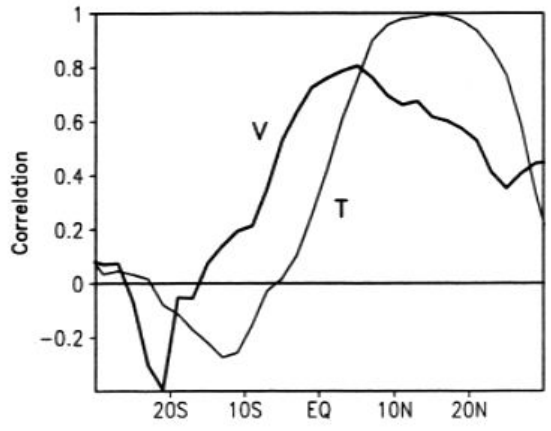

Figure 2 Cross-correlation with northern tropical (10N-20N) SST for 1964-93: SST (thin) and meridional wind velocity (thick curve) based on COADS 60W-20E zonal means. No temporal filter is applied.

2. Model

The tropical climate system contains two types of ocean-atmosphere interaction: the Bjerknes (1969) and wind-evaporation-SST (WES; Xie and Philander 1994) feedbacks. Ocean GCM simulations suggest that they are responsible for the equatorially symmetric monopole (Huang et al. 1995) and anti-symmetric dipole (Carton et al. 1996) modes in the Atlantic, respectively. These feedback mechanisms have been studied separately. Our experience with each of these mechanisms has accumulated to such a point that it is now possible to construct a unified model to include both.

For the atmosphere we adopt the Matsuno (1966)-Gill (1980) model with SST as forcing. Such a dynamic formulation requires spatial modal patterns to be determined by internal dynamics, unlike previous semi-empirical models imposing them *a priori* from observations (Chang et al. 1997). This is an important difference given we are concerned with the physical basis for modal decomposition. Such a dynamic model further allows calculating dispersion relations for the first time, an advantage to become crucial in the Pacific-Atlantic comparison.

The ocean is a linearized version of the Zebiak-Cane (1989) model, where SST (T) is affected by upwelling, horizontal advection and surface heat flux:

$$T_t + \bar{\mathbf{u}}\cdot\nabla T + \mathbf{u}\cdot\nabla\bar{T} = aU - [\mathbf{b} + H(\bar{w})\bar{w}/D_e]T + [\bar{w}\dot{T}_e h - w(\bar{T} - \bar{T}_e)]H(\bar{w})/D_e + \kappa\nabla^2 T \ .$$

Here, the subscript t denotes the local time derivative, the overbar the basic state variables, the prime denoting perturbation is omitted, $\mathbf{u}$ and w are horizontal and vertical velocities, D_e is the depth at which water is entrained into the mixed layer, H(w) is the Heaviside function and κ is the diffusivity. The entrainment temperature $T_e(h)$ is a function of thermocline depth (h) determined by solving the reduced gravity equations, and $\dot{T}_e$ its derivative. See Neelin et al. (1998) for the model's ENSO applications. Here we add a wind-speed (U) dependent evaporation term—the first on the rhs—to the original Zebiak-Cane model, thus incorporating both the Bjerknes and WES feedbacks. The WES and Newtonian cooling terms result from linearizing the latent heat flux term, with a and b being their respective coefficients (Xie 1996). The basic state is zonally uniform but varies in the meridional direction. In particular, upwelling effects are confined to a narrow equatorial zone as in observations. The basic state is made symmetric about the equator but is otherwise typical of the Pacific and Atlantic, with easterly trades driving poleward Ekman flows in the ocean.

The model equations are solved by time-stepping under zonally cyclic conditions. For a given zonal wavenumber, time integration is carried out until steady exponential trends in perturbation amplitude are established. Such wave solutions prove useful for understanding the coupled oscillation in an enclosed ocean basin (Neelin et al. 1998). Land surface and ocean boundary effects are left for future studies.

3. Modal Structure and Dispersion Relation

In the model arbitrary initial disturbances disperse into two sets of modes: equatorially symmetric and anti-symmetric, respectively, in support of our empirical decomposition. As

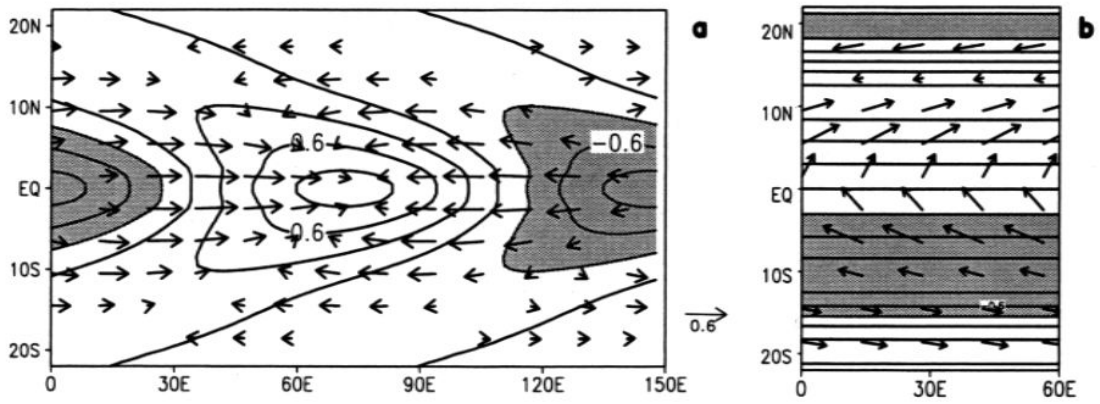

Figure 3 Dominant modes at **a**, the Pacific and **b**, the Atlantic wavelengths in the coupled model. SST in contours (<-0.3°C shaded) and surface wind velocity (m/s) in vectors.

will be explained below, the type of dominant mode and its horizontal structure vary with zonal wavelength (Fig. 3). The frequencies of the symmetric and dipole modes are well separated: The former prefers interannual time scales whereas the latter exhibits lower frequencies (Fig. 4a), a result consistent with observations (Servain 1991).

The equatorially symmetric mode is due to the Bjerknes feedback. A positive SST anomaly induces anomalous westerly winds to the west (Fig. 3a), which depress the thermocline to the east. The depressed thermocline increases the subsurface temperature upwelled into the mixed layer, enhancing the initial SST anomaly. Meanwhile the westerly anomalies reduce upwelling velocity and cause the coupled disturbance to move westward. On the other hand, the WES feedback is responsible for the anti-symmetric mode. The interhemispheric SST gradient with a positive (negative) anomaly north (south) of the equator drives cross-equatorial southerly winds, which the Coriolis force turns toward the east (west) in the Northern (Southern) Hemisphere (Fig. 3b). Thus induced zonal wind anomalies, superimposed on mean easterly trades in the basic state, reduce (enhance) total wind speed and evaporation north (south) of the equator, amplifying the initial SST dipole.

The symmetric and dipole modes display very different growth rate dependence on zonal wavenumber (Fig. 4b). The latter's growth rate decreases monotonically with wavenumber while the former's has an optimal wavelength near the Pacific size (L=150° longitude) where the maximum growth is achieved. The symmetric mode becomes subcritical at the Atlantic size (L=60°). The growth rate itself and the optimal wavelength varies slightly with different basic states, but the shape of the growth curve remains unchanged. This difference between the symmetric and dipole modes has an important consequence to climate variability in ocean basins of different zonal sizes. For the large Pacific, the equatorial mode is supercritical so a self-sustaining ENSO cycle dominates. At the small Atlantic wavelength (k=1), on the other hand, the monopole and the k=0 dipole modes have comparable growth rates, making them both visible in the model simulation.

The different growth characteristics between the Bjerknes and WES instabilities arise from their differences in growing mechanism. The symmetric mode owes its growth to the interaction of zonal wind, SST and upwelling near the equator. In the Matsuno-Gill model, it can be shown that at either the long or short wave limit, equatorial zonal winds are 90° out of phase with SST forcing. So the Bjerknes feedback is very weak or non-existent. Only at finite wavelengths, equatorial zonal wind has an in-phase component with the SST, causing the coupled disturbance to grow. As a result, we see a growth rate maximum at a finite wavelength. The WES feedback, in contrast, involves ocean-atmosphere interaction in the meridional direction. In the presence of zonal variations, the phase difference between wind speed and SST induces zonal

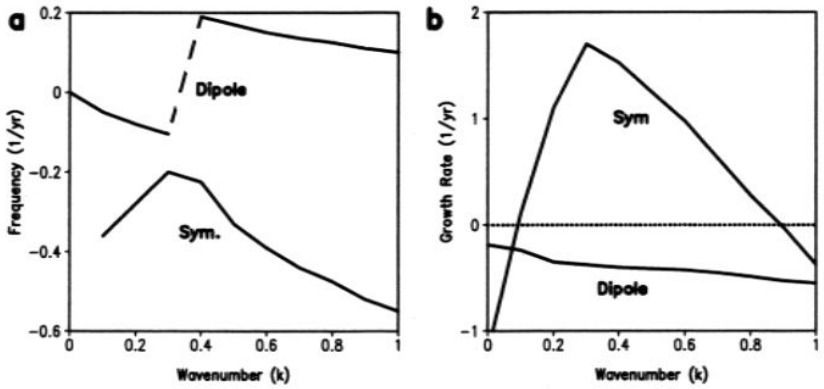

Figure 4 Dispersion relation of dominant coupled modes: **a**, Frequency (1/period) and **b**, growth rate as a function of zonal wavenumber (normalized by the Atlantic wavelength L=60°). The least damped dipole mode transfers from a westward to an eastward propagating one as wavenumber increases.

phase propagation at the expense of amplitude growth (Xie 1996). Thus the dipole's growth rate peaks at k=0 and decreases with wavenumber. This seems to explain why the observed Atlantic dipole is largely zonally uniform.

Finally we note an increase in meridional scale of the symmetric mode from the Pacific to Atlantic wavenumber (not shown), a result consistent with the observation that the Pacific ENSO is equatorially trapped whereas the Atlantic monopole shows little meridional structure within 20° latitudes (Tanimoto and Xie 1999). A slowly growing mode has a broad meridional structure because the mean Ekman flow can advect farther poleward SST anomalies generated in the equatorial upwelling zone. As the equatorial Bjerknes feedback weakens at large wavenumbers, relative importance of the zonal WES feedback (Zhou and Carton 1998) increases, further reducing the equatorial trapping.

4. Discussion

The difference between the Bjerknes and WES feedbacks revealed here can help understand the differences between the Pacific and Atlantic variability. The Bjerknes feedback is possible only within a narrow equatorial upwelling zone, whereas the WES feedback is effective in the off-equatorial regions where Ekman downwelling shuts off subsurface effects on SST and thermocline variability reduces to a passive response to varying winds. While the former feedback is so strong as to obscure the latter in the Pacific, the small size of the Atlantic allows the weaker WES feedback to compete and manifest itself as a dipole SST mode. The ITCZ, which requires the underlying total SST to exceed a critical value, may act as a nonlinear mode selector. In the Pacific a major El Nino can move the ITCZ toward the equator while the Atlantic SST monopole appears too weak in amplitude to affect the ITCZ (Servain et al. 1999). It is the dipole that with its interhemispheric SST gradient, moves the Atlantic ITCZ north-southward, most pronouncedly in boreal spring when the seasonal warming occurs on the otherwise cold equator (Nobre and Shukla 1996). With its deep vertical structure, variability in the ITCZ can impact the large-scale atmosphere (Rajagopalan et al. 1998; D. Battisti 1997, personal communication), helping organize climate variability in both the Tropics and extratropics.

In reality, neither the Bjerknes nor WES feedback is strong enough to cause a supercritical instability in the Atlantic. Such a lack of unstable modes may be responsible for the difficulty in detecting physical modes in the Atlantic. External forcing is therefore needed to excite the monopole and dipole (Zebiak 1993; Chang et al. 1997). As the least damped modes, they act to organize the forced response into their preferred time-space patterns. Thus the observed tropical Atlantic variability is likely to reflect local ocean-atmosphere interactions we focus here as well as time-space characteristics of forcings by the extratropical NA (Xie and Tanimoto 1998) and equatorial Pacific (Enfield and Mayer 1997).

Acknowledgments. We thank J. McCreary for constructive comments, K. Trenberth and A. Kitoh for helpful discussions. Supported by grants from the Education Ministry (SPX), the Science and Technology Agency (YT & TM) and the Asahi Beer Foundation for the Promotion of Science (SPX).

References

Bjerknes, J. Atmospheric teleconnections from the equatorial Pacific. *Mon. Wea. Rev.* **97**, 163-172 (1969).

Carton, J., et al. Decadal and interannual SST variability in the tropical Atlantic Ocean. *J. Phys. Oceanogr.* **26**, 1165-1175 (1996).

Chang, P., L. Ji and H. Li, A decadal climate variation in the tropical Atlantic ocean from thermodynamic air-sea interactions. *Nature* **385**, 516-518 (1997).

Deser, C. and M.L. Blackmon, Surface climate variations over the North Atlantic Ocean during winter. *J. Clim.* **6**, 1743-1753 (1993).

Enfield, D.B. and D.A. Mayer, Tropical Atlantic SST variability and its relation to El Nino-Southern Oscillation. *J. Geophys. Res.* **102**, 929-945 (1997).

Gill, A.E. Some simple solutions for heat-induced tropical circulation. *Q. J. R. Meteor. Soc.* **106**, 447-462 (1980).

Houghton, R.W. and Y.M. Tourre, Characteristics of low-frequency sea surface temperature fluctuations in the tropical Atlantic. *J. Clim.* **5**, 765-771 (1992).

Huang, B., J.A. Carton and J. Shukla, A numerical simulation of the variability in the tropical Atlantic Ocean, 1980-88. *J. Phys. Oceanogr.* **25**, 835-854 (1995).

Kushnir, Y., Interdecadal variation in North Atlantic sea surface temperature and associated atmopheric conditions. *J. Clim.* **7**, 141-157 (1994).

Matsuno, T. Quasi-geostrophic motions in the equatorial area. *J. Meteor. Soc. Jpn* **44**, 25-43 (1966).

Mehta, V.M. Variability of the tropical ocean surface temperatures at decadal-multidecadal time scales. Part I: The Atlantic Ocean. *J. Clim.* **11**, 2351-2375 (1998).

Neelin, J.D. et al. ENSO theory. *J. Geophys. Res.* **103**, 14261-14290 (1998).

Nobre, P. and J. Shukla, Variations of sea surface temperature, wind stress, and rainfall over the tropical Atlantic and South America. *J. Clim.* **9**, 2464-2479 (1996).

Rajagopalan, et al. Observed decadal midlatitude and tropical Atlantic climate variability. *Geophys. Res. Lett.* **25**, 3967-3970.

Servain, J. Simple climate indices for the tropical Atlantic Ocean and some applications. *J. Geophys. Res.* **96**, 15137-15146 (1991).

Servain, J. et al., Relationship between the equatorial and meridional modes of climatic variability in the tropical Atlantic. *Geophys. Res. Lett.* **26**, 485-488 (1999).

Tanimoto, Y. and S.-P. Xie, Ocean-atmosphere variability over the pan-Atlantic basin. *J. Meteor. Soc. Jpn* **77**, 31-46 (1999).

Venegas, et al. Atmosphere-ocean coupled variability in the South Atlantic. *J. Clim.* **10**, 2904-2920 (1997).

Xie, S.-P. Westward propagation of latitudinally asymmetry in a coupled ocean-atmosphere model. *J. Atmos. Sci.* **51**, 3236-3250 (1996).

Xie, S.-P. and Y. Tanimoto, A pan-Atlantic decadal climate oscillation. *Geophys. Res. Lett.* **25**, 2185-2188 (1998).

Xie, S.-P. and S.G.H. Philander, A coupled ocean-atmosphere model of relevance to the ITCZ in the eastern Pacific. *Tellus* **46A**, 340-350 (1994).

Zebiak, S.E. Air-sea interaction in the equatorial Atlantic region. *J. Clim.* **8**, 1567-1586 (1993).

Zebiak, S.E. and M.A. Cane, A model of El Nino-Southern Oscillation. *Mon. Wea. Rev.* **115**, 2262-2278 (1989).

Zhou, Z. and J.A. Carton, Latent heat flux and interannual variability of the coupled atmosphere-ocean system. *J. Atmos. Sci.*. **55**, 494-501 (1998).

S.-P. Xie, H. Noguchi, Graduate School of Environmental Earth Science, Hokkaido University, Sapporo 060-0810, Japan (e-mail: xie@ees.hokudai.ac.jp; hideyo@ees.hokudai.ac.jp)

Y. Tanimoto, T. Matsuno, Frontier Research System for Global Change, 1-2-1 Shibaura, Minato, Tokyo 105-6791, Japan (e-mail: tanimoto@frontier.esto.or.jp)

(Received February 18, 1999; revised April 7, 1999; accepted April 13, 1999)